ACTA METALLURGICA SLOVACA
2026, VOL. 32, NO. 3, 262-266

RESEARCH PAPER

Damping Behavior of Cr–Si–La–Mn Alloy Steels and Structural Characteristics of Nanostructured TiN–Ni Coatings

Rysbubi Zh. Abuova[1], *Gulziya A. Burshukova*[1,2]*, *Yerik S. Merkibayev*[1]

[1]International educational corporation, Ryskulbekova str 28, 050043, Almaty, Kazakhstan
[2]Satbayev University, Satpayev str 22, 050013, Almaty, Kazakhstan

**Corresponding author: gulziya.burshukova@gmail.com, tel:+77012559144, Satbayev University, Satpayev str 22, 050013, Almaty, Kazakhstan.*

Received: 30.06.2026
Accepted: 21.09.2026

ABSTRACT

This article presents results from a comprehensive study of newly developed Cr-Si-La-Mn alloy steels with enhanced damping properties for operation under dynamic and vibration loading conditions. The research focuses on increasing the vibration energy dissipation capacity of structural steels by forming multifunctional nanostructured ceramic-metallic coatings on their surfaces. To further improve damping characteristics, the researchers deposited TiN-Ni coatings with different nickel contents on steel substrates by ion-plasma vacuum-arc deposition. The study investigated how coating composition and deposition parameters affect the structural evolution, phase composition, morphology, and functional properties of the coating-substrate system. The deposited coatings had a dense nanostructured architecture consisting of titanium nitride phases and a metallic nickel component, which enhances energy dissipation mechanisms. The study demonstrates that the damping behavior of coated steels is governed not only by the intrinsic damping capacity of the substrate and coating materials but also by additional dissipation mechanisms arising at the coating-substrate interface. These mechanisms include interfacial friction, microplastic deformation, stress redistribution, dislocation interactions, and elastic-wave scattering at phase and structural boundaries. A nanostructured coating significantly increases the material's ability to absorb and dissipate mechanical vibration energy. Comparative analysis of uncoated and coated specimens revealed that TiN-Ni coatings substantially improve the acoustic and damping characteristics of the developed steels. The highest damping performance was achieved for coatings with an optimized nickel content, providing an effective combination of hardness, wear resistance, and vibration attenuation. The results indicate that the proposed coating-substrate systems are promising for machine-building, power engineering, transport, and other applications that require high mechanical strength, wear resistance, noise reduction, and vibration suppression.

Keywords: damping steel, Cr–Si–La–Mn alloy, internal friction, TiN–Ni coating, acoustic properties, vacuum-arc deposition.

INTRODUCTION

Impact noise is the most widespread and harmful industrial factor in manufacturing industries. One of the high-performance and effective sectors is metallurgy, which, however, is characterized by a high level of noise and vibration. Industrial noise and sound vibrations worsen working conditions and negatively affect workers' health. Intense vibration damages machine and mechanism structures, reducing their service life. These problems present engineers and technologists with the task of reducing noise and vibration levels. Noise and vibration in production are harmful and dangerous factors that negatively impact workers' health. These factors have a common mechanical oscillatory nature, and their influence can lead to various diseases. Such diseases include hearing disorders (sensorineural hearing loss), musculoskeletal disorders (vestibular syndrome, polyneuropathy of the upper and lower limbs), as well as cardiovascular diseases (angiodystonic syndrome). These pathologies can develop with prolonged exposure to vibroacoustic factors whose levels exceed established workplace hygiene standards [1-3].

Any noise creates a load on the human nervous system. Its effects vary depending on age, health status, the nature of work, and physical and emotional conditions. An interesting psychological feature is that noise generated by a person does not bother them, while external noise causes strong irritation. Prolonged exposure to noise can lead to the development of diseases such as neuroses, hypertension, peptic ulcers, and skin and intestinal disorders [1-3]. One of the most prominent symptoms of the development of vibration disease in workers is angiodystonic syndrome. It is characterized by periodic spasms of the blood vessels in the hands and feet (Raynaud's syndrome [2]). The skin on the fingers and sometimes the feet turns white. Initially, this occurs when washing hands with cold water or during overcooling. Over time, blood supply insufficiency in the fingertips develops, which can lead to cyanosis and tissue necrosis (**Fig. 1**).

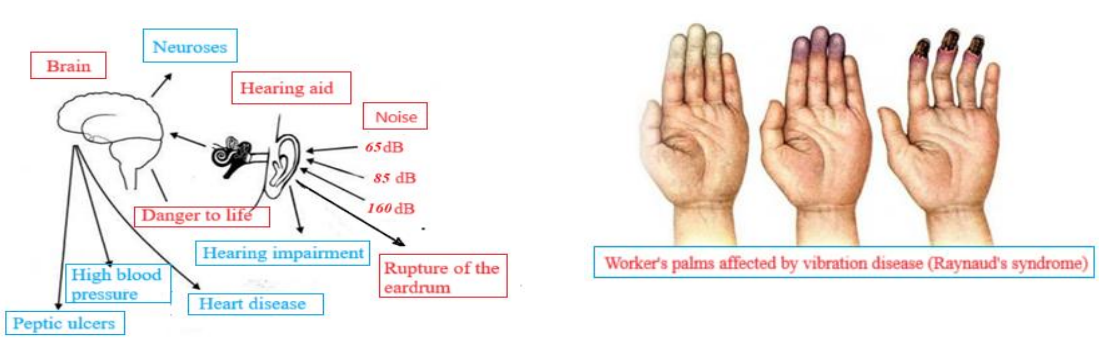

A) B)

Fig. 1 Impact of Noise and Vibration on the Human Body

In metallurgical production, impact and tonal noises often prevail and are considered the most harmful to workers' health. Short impulse noises increase the likelihood of hearing loss [1,3].
To reduce noise levels at its source, it is necessary to replace impact processes with non-impact processes, substitute metallic materials with non-metallic ones, and employ other methods that can effectively combat noise levels [3]. The most effective method for reducing noise at its origin is the use of damping materials. Non-metals (plastics, wood, polyethylene, etc.) and non-ferrous metals can be used. However, the most relevant approach for reducing noise in stamping production is the use of damping metallic materials based on iron [4-8].
The damping capacity of a metallic matrix depends on the degree of microplastic deformation within it, which is associated with its structure and mechanical properties. Damping is maximized when the structure is ferritic. Damping is lowest with a pearlitic structure. A mixed structure demonstrates intermediate properties. A mixture of ferrite and troostite exhibits poorer characteristics than pearlite because of the presence of ferrite. Hardened steel with a martensitic structure has stronger damping properties than troostite, related to increased dislocation density and the formation of excessive stresses at the ends of martensitic crystals [4-8].
In the majority of technological processes, the use of non-metallic damping materials is limited due to their insufficient strength properties. Therefore, the creation of iron-based alloys with enhanced damping ability, achieved by altering their chemical composition and employing special heat treatments, becomes highly relevant. However, modification of structural materials through coating deposition is rarely applied [9].
Improvement of the operational characteristics of products through the application of standard coatings, such as chromium plating and nitriding, has nearly exhausted its possibilities. This situation requires innovative approaches to the development and improvement of a new generation of functional coatings that possess increased resistance to failure under cyclic thermomechanical loads and aggressive environments. One of the directions for this work is the creation of nanostructured coatings. Nanostructured materials with a high area of grain boundaries exhibit high toughness and resistance to the initiation and development of "brittle" cracks. They can resist destruction for extended periods under complex external stress. The design of the next generation of nanostructured composite coatings, with high areas of grain boundaries, allows for the development of a combination of high physicochemical properties [10-11].

MATERIALS AND METHODS

Alloy design and preparation

Three experimental alloys designated EO-1, EO-2, and EO-3 were produced and compared with conventional cast steels 15L, 25L, 35L, and 50L. Metallic charge materials included metal scrap, ferroalloys, production waste, and Armco iron. Melting was carried out in a crucible induction furnace. The steel`s purpose and nominal compositions used in the experiments are listed in **Tables 1 and 2**, respectively.

Table 1 Purpose and General Characteristics [12]

Steel	Purpose
15L	Parts subjected to impact loads (e.g., tapping hammers, grabs, blocks, rollers) and sharp temperature fluctuations (e.g., molds of casting machines, furnace fittings, slag pots, tuyeres of the casting machines in the open hearth shop, boxes and trays for annealing sheets), as well as welded-cast structures with large volumes of welding.
25L	Beds of rolling mills, pulleys, traverses, pistons, molds, bearing housings, gears, steam turbine fittings, axles, shafts, steam hammer hammers, and other parts operating under the influence of medium static and dynamic loads. Parts made from steels 20L and 25L can operate under pressure at temperatures ranging from -40 to +450°C. The steel is not sensitive to overheating.
35L	Housings and casings of turbo machines, beds of rolling mills, steam hammer hammers, parts of turbine drills, valves, diaphragms, forks, brackets, and other components operating under the influence of medium static and dynamic loads. The steel is used in an improved condition and after surface hardening by high-frequency heating (HF).
50L	Gears, runners, wheels, toothed rims, toothed couplings of hoisting and transport machines, drive wheels, and rollers of heavy, medium, and light section mills for rolling soft metals. The steel is used in a normalized and improved condition and after surface hardening with high-frequency heating (HF).

Table 2 Chemical composition of the investigated steels, wt.%

Alloy	C	Si	Mn	Cr	La	Ca	S (max)	P (max)	Cu
15L	0.12–0.20	0.20–0.52	0.30–0.90	≤0.30	–	–	0.045	0.040	0.30
25L	0.22–0.30	0.20–0.52	0.35–0.90	≤0.30	–	–	0.045	0.040	0.30
35L	0.32–0.40	0.20–0.52	0.40–0.90	–	–	–	–	–	–
50L	0.47–0.55	0.20–0.52	0.40–0.90	0.30	–	–	0.045	0.040	0.20–0.30
EO-1	0.30	0.40	0.80	1.00	0.12	0.15	0.045	0.040	0.30
EO-2	0.40	0.50	0.75	1.00	0.15	0.18	0.045	0.040	0.30
EO-3	0.50	0.45	0.90	1.00	0.21	0.20	0.045	0.040	0.30

Standard cast steels were retained as reference materials, as they provide a practical basis for assessing whether newly developed compositions maintain the required levels of strength and impact toughness while altering damping-related characteristics. The EO series involves a gradual increase in carbon content from 0.30 to 0.50 wt.% and lanthanum (La) from 0.12 to 0.21 wt.%, with smaller variations in silicon (Si) and manganese (Mn). The chromium content in all three EO alloys remained at 1.00 wt.%. This design allows for a comparison of the combined effect of compositional changes, but it does not constitute a single-factor experiment for La.
The experimental process consisted of four sequential stages: (i) preparation and comparison of the composition of EO alloys with standard casting steels; (ii) evaluation of mechanical properties; (iii) measurement of impact toughness and damping for the set of alloys; and (iv) selection of EO-3 for surface modification with TiN-Ni, followed by a pairwise comparison of EO-3 before and after coating.

Mechanical characterization

The mechanical characteristics considered in the comparison included yield strength (σ0.2), impact toughness (KCU), elongation (δ5), reduction of area (θ), and tensile strength (σB). **Table 3** includes only the values specified in the original dataset; empty rows from the earlier manuscript were removed rather than interpreted.
The mechanical property data were interpreted as selection criteria rather than as evidence that every EO alloy must outperform any standard steel. This distinction is important because high-damping structural materials must retain sufficient load-bearing capacity, yet the optimal material is expected to represent a compromise between strength, ductility, impact toughness, acoustic characteristics, and damping-related parameters.
For the comparative analysis, values for the EO series were evaluated against available data for the 15L and 25L grades. The study excluded the 35L and 50L grades from the quantitative comparison because the earlier manuscript reported incomplete mechanical property data and the original dataset lacked verified values.

Table 3. Mechanical properties reported for the reference and experimental steels

Alloy	σ0.2, MPa	KCU, J/cm²	δ5, %	ψ, %	σB, MPa
15L	200	50	24	35	400
25L	240	40	19	30	450
EO-1	220	45	19	30	460
EO-2	230	50	20	35	440
EO-3	210	45	21	35	480

Acoustic and damping measurements

Plate specimens measuring 50×50×5 mm were investigated using an impact excitation setup. Steel impact spheres with diameters of 7, 8, 9, and 11 mm and corresponding masses of 1.40, 2.09, 2.97, and 5.55 g were used. Each sphere rolled down an inclined plane and struck the geometric center of the suspended specimen without obstruction. Sound emission was recorded using an OKTAVA-101A sound level meter (**Fig. 2**), while vibration was measured using a Brüel & Kjær Model 2204 instrument.

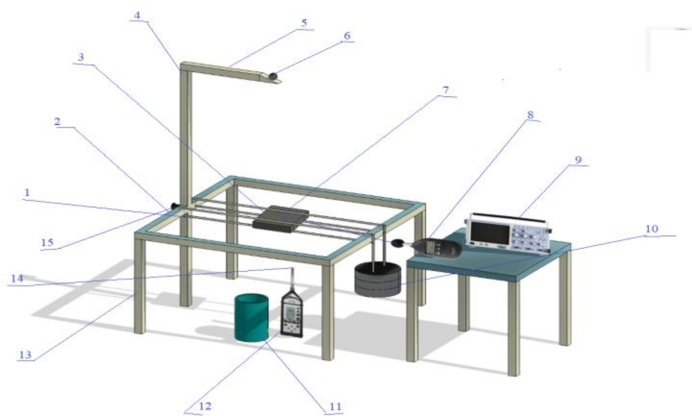

Fig. 2 Device for comprehensive acoustic investigation [13]: 1 - capron threads; 2 - frame; 3 - sample plate; 4 - frame stand; 5 - inclined plane; 6 - ball impactor; 7 - vibration sensor of the Bruel & Kjer sound level meter; 8 - Bruel & Kjer sound level meter model 2204 with octave filter model 1613; 9 - S-18 oscilloscope; 10 - load; 11- ball receiver; 12 - «Octava101A» sound level meter; 13 - framestands; 14 - microphone of the «Octava101A» sound level meter; 15 - screw for securing the impactor stan

The specimen was suspended by nylon threads to minimize the influence of a rigid support and to minimize support effects and ensure reproducible boundary conditions during free vibration after impact. The impact height was adjusted using a mechanical device mechanism. Using spheres of different masses made it possible to vary the excitation amplitude while maintaining the same basic impact geometry.

Sound pressure levels were measured in octave bands ranging from 31.5 to 31,500 Hz. Five measurements were taken for each acoustic condition, and the arithmetic mean value was used. Calibration was performed using a ZG-10 sound generator and a PF-101 pistonphone, with laboratory temperature and humidity maintained at constant levels.

Sound level measurements characterize the acoustic response of the specimen under impact loading. Therefore, they should be distinguished from material parameters derived from the shape of the decaying signal. In this analysis, the A-weighted sound level is treated as a technical vibroacoustic indicator, whereas the logarithmic decrement and internal friction parameter are regarded as damping-related quantities derived from the transient response.

The decay of the acoustic pulse following impact was recorded using an oscilloscope. The logarithmic decrement was determined based on the reduction in oscillation amplitude according to the formula $\delta = (1/n)\ln(A0/An)$, where A0 is the initial amplitude, an is the amplitude after n oscillations, and n is the number of oscillations considered. Relative energy dissipation and internal friction were estimated using the same methodology previously employed by the authors [14].

The logarithmic decay coefficient represents the rate at which the oscillation amplitude decreases over successive cycles. Since the energy of linear oscillations is proportional to the square of the amplitude, a decrease in amplitude can be attributed to energy dissipation during a cycle. The relative energy dissipation parameter and the magnitude of internal friction were calculated using the methodology applied in a previous study within the project [14]. The same method was used here to ensure comparability across all stages of the project.

TiN–Ni coating deposition and characterization

The EO-3 alloy was selected for surface modification with a nanostructured TiN–Ni cermet coating (CMNC). The coating was deposited using a Bulat HNV-6.6-I3 vacuum-arc ion-plasma system (**Fig. 3**). VT1-0 titanium (containing approximately 99.5% Ti) and Ti–Ni composite cathode materials produced via powder metallurgy served as the starting materials. The deposition procedure comprised substrate preparation, ion cleaning and heating, coating deposition, and cooling. Available structural data were used to evaluate crystallite refinement, phase evolution, coating morphology, and porosity.

The term CMNC (ceramic-metal nanostructured coating) is used in the revised manuscript to designate the TiN-Ni surface layer. Thus, EO-3/CMNC refers to the EO-3 substrate after TiN-Ni deposition, whereas EO-3 refers to the corresponding uncoated alloy. This designation replaces the earlier abbreviation KMNP, which was not readily understood by an international audience.

The coating process involved substrate preparation, ion cleaning and heating, vacuum-arc deposition, and controlled cooling. During vacuum-arc deposition, Ti and Ti-Ni cathode materials supplied the metal flux, while nitrogen formed the nitride phase. The Bulat system also separates ion flux and substrate biasing, factors that can influence macroparticle density and coating densification.

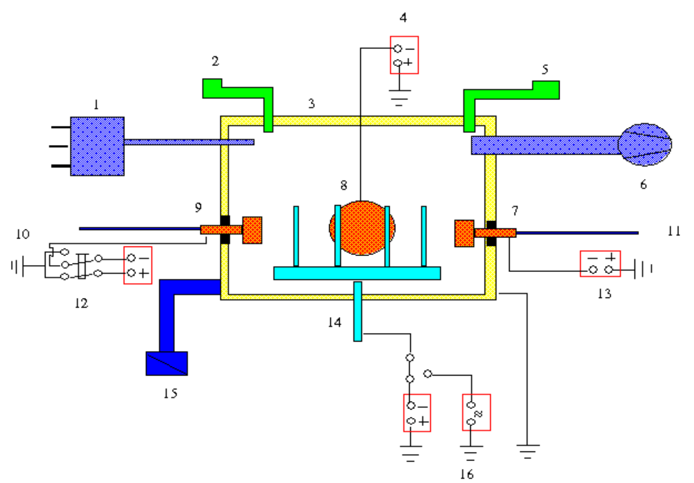

Fig. 3 Principle of operation of the universal vacuum-arc system [13]: 1 - gas mixer; 2 - vacuum gauge; 3 - chamber of the system;4 - power source for the accelerator-separator; 5 - temperature control system;6 - vacuum system;7, 9 - arc evaporators; 8 - source of separated plasma; 10, 11 - cooling systems for the evaporators; 12, 13 - power sources for the evaporators;14 - rotary table for placing the tool;15 - heating and cooling system for the chamber;16 - source of pulsed bias voltage applied to the tool

RESULTS AND DISCUSSION

Mechanical properties of the experimental alloys

Mechanical results indicate that the EO series alloys retain a useful range of structural properties while shifting the balance between yield strength, tensile strength, ductility, and impact toughness. EO-1 exhibited a yield strength of 220 MPa and a tensile strength of 460 MPa; EO-2 showed 230 MPa and 440 MPa, respectively; and EO-3 showed 210 MPa and 480 MPa. Elongation increased from 19% for EO-1 to 21% for EO-3, while the reduction of area was 30% for EO-1 and 35% for both EO-2 and EO-3. EO-2 possesses the highest impact toughness in the EO series at 50 J/cm².

Compared to the 15L alloy, EO-3 demonstrated a 20% higher tensile strength (480 vs. 400 MPa), while EO-1 and EO-2 also exceeded the tensile strength of the 15L alloy. However, the yield strength of EO-3 remained lower than that of the 25L alloy, and the yield strength of EO-2 did not exceed that of the 25L alloy. Thus, the data do not support a generalized claim that all mechanical properties improved simultaneously. Instead, the experimental compositions offer various combinations of strength and ductility that must be considered alongside vibroacoustic characteristics.

This trade-off is significant for material selection. A damping alloy intended for machine components cannot be optimized solely for low noise radiation or high damping capacity if this comes at the expense of load-bearing capabilities. Therefore, comparing the EO series served as a screening step before surface modification.

Damping and acoustic characteristics

The measurement result for 15L serves as a useful benchmark for interpreting the vibration attenuation method: $\delta = 0.014$, $\psi = 0.028$, and $Q^{-1} = 0.004$. These values describe the short-term attenuation observed under the test conditions and should not be directly equated to the A-weighted sound level measured upon impact. The earlier manuscript conflated these concepts, leading to an oversimplified interpretation of the results.

A comparative dataset for uncoated alloys is presented in **Table 4**. EO-3 exhibited the highest measured internal friction value among the EO series alloys (31.245×10^{-4}), whereas EO-1 and EO-2 showed values of 18.281×10^{-4} and 16.268×10^{-4}, respectively. Noise levels did not follow the same order, demonstrating that it is impossible to establish a simple monotonic relationship between the specified internal friction parameter and the A-weighted sound level.

In the EO series, internal friction values were 18.281×10^{-4} for EO-1, 16.268×10^{-4} for EO-2, and 31.245×10^{-4} for EO-3. Thus, EO-3 exhibited internal friction approximately 71% higher than EO-1 and approximately 92% higher than EO-2. Meanwhile, A-weighted noise levels were 63, 68, and 70 dBA, respectively. This difference in ranking indicates that the internal friction parameter and impact noise level cannot be considered interchangeable indicators of damping.

Reference steels demonstrate a similar lack of simple ranking. For example, 35L steel had a noise level of 54 dBA with an internal friction value of 24.120×10^{-4}, whereas 50L steel registered 75 dBA with a value of 25.110×10^{-4}. The relatively small difference in internal friction, compared to the much larger difference in sound level, suggests that impact-induced acoustic radiation is additionally governed by stiffness, modal properties, radiation efficiency, and contact response.

Table 4 Internal friction, experimental dispersion, and sound level of the investigated alloys

Alloy	Internal friction $Q^{-1} \times 10^4$	Experimental dispersion $S^2 \times 10^4$	Sound level, dBA
15L	26.136	0.5760	63
25L	25.026	0.5566	65
35L	24.120	0.7840	54
50L	25.110	0.9900	75
EO-1	18.281	0.4770	63
EO-2	16.268	0.5884	68
EO-3	31.245	1.8880	70

Effect of the TiN–Ni CMNC on the vibroacoustic response of EO-3

Sample EO-3 was examined before and after application of a metal-ceramic nanostructured TiN-Ni coating. The uncoated EO-3 alloy exhibited a noise level of 70 dBA and a reported internal friction value of 31.245 x 10^-4. After surface modification, EO-3/CMNC exhibited a noise level of 56 dBA and an internal friction value of 14.281 × 10^-4. Thus, the coating reduced the measured A-weighted noise level by 14 dBA (**Table 5**). Because the decibel scale is logarithmic, a 14 dB change represents a substantial reduction in the measured impact sound level.

Table 5 Paired vibroacoustic characteristics of EO-3 before and after TiN–Ni coating deposition

Sample	Surface state	Internal friction $\times 10^4$	Sound level, dBA	Change in sound level
EO-3	Uncoated	31.245	70	–
EO-3/CMNC	TiN–Ni coated	14.281	56	−14 dBA

The internal friction parameter changed in the opposite numerical direction, decreasing by approximately 54%. This result is important because it prevents the coating effect from being described as a simple increase in internal friction. Instead, the paired experiment demonstrates a noticeable change in the overall vibroacoustic response of the EO-3/CMNC system. The coating can influence contact stiffness, surface stress distribution, modal response, and acoustic emission, in addition to any contribution to internal energy dissipation.

For engineering applications, reducing noise emission is important in its own right, as machine components are often selected not only for their intrinsic damping but also for their ability to reduce impact noise at the source. However, scientific interpretation must distinguish between acoustic emission and internal friction. Future experiments that test coated and uncoated specimens under identical deformation conditions (operating mode and amplitude) will help quantify how much of the 14dBA reduction is attributable to intrinsic damping versus altered surface or contact response.

Structural characteristics of TiN–Ni coatings

Vacuum-arc deposition of TiN-Ni significantly refined the nitride phase. According to available structural data, the characteristic size of TiN crystallites decreased from approximately 100–110 nm to about 15 nm as the metallic component was varied. It has been reported that at Ni contents below 12 at.%, the Ni remains X-ray amorphous; as the Ni concentration increases, the TiNi intermetallic phase forms, and the deposited layer becomes more porous. SEM observations revealed a predominantly columnar coating morphology, with structural units oriented approximately perpendicular to the substrate surface.

Crystallite refinement increases the volume fraction of grains and phase boundaries within the coating. From a mechanical standpoint, such boundaries can influence hardness, crack propagation, local plasticity, and stress transfer. However, their direct contribution to damping cannot be quantitatively assessed based on morphology alone. Thus, while structural observations are used in this study to describe the coating's state, no specific energy dissipation mechanism is proposed without further evidence.

These observations are consistent with recent research on TiN-based coatings. Akhter et al. reported that the introduction of Ni alters phase composition, nanocomposite formation, and hardness, with the nanocomposite structure developing at intermediate Ni contents [10]. The same authors demonstrated that increasing the negative substrate bias can lead to coating densification and a reduction in macroparticle density, while simultaneously altering the mechanical response [11]. These results support the premise that the coating structure observed in the present study is sensitive to both composition and deposition parameters, and that precise processing conditions should be specified when comparing coating characteristics.

Interpretation of the coating–damping relationship

An earlier version of the manuscript stated that TiN-Ni coatings significantly increase damping, attributing this effect to quasi-free dislocations, point and line defects, and interfacial stress fields. The sample identification has now been clarified: the coated sample is EO-3. This enables a direct "before-and-after" comparison and confirms a substantial reduction in radiated sound levels from 70 to 56 dBA. However, the internal friction parameter simultaneously decreased from 31.245×10^{-4} to 14.281×10^{-4}. Thus, while the experimental data confirm a significant shift in vibroacoustic characteristics resulting from the coating application, they do not support the more specific claim that the coating enhanced damping simply by increasing internal friction.

One possible explanation for the discrepancy between sound level and internal friction is that these measurements probe different aspects of the response. Internal friction is governed by damping behavior and relates to energy loss within the vibrating system, whereas impact noise levels also depend on acoustic radiation efficiency and the duration of contact. A hard-nanostructured coating can alter local contact stiffness and surface stress distribution, even if the bulk substrate remains unchanged. Such changes can modify the frequency spectrum and radiation efficiency upon impact.

Micro-alloying with rare-earth elements adds another layer of complexity to material design. Literature indicates that rare-earth additions can modify inclusions, interfaces, carbide morphology, and internal friction characteristics [15,16]. However, because the EO-1 through EO-3 compositions differ in C, Si, Mn, and La content simultaneously, the current dataset does not allow isolation of La as the sole cause of the observed differences. In a future dedicated experiment, keep the concentrations of C, Si, Mn, and Cr constant while varying only the La concentration.

Dislocation-based damping remains a physically plausible mechanism in iron-based alloys, and the classical Granato-Lücke theory, combined with more recent studies on Fe-Mn, provides the theoretical basis for such an interpretation [4, 17].

CONCLUSION

- Three experimental Cr-Si-La-Mn steels (EO-1, EO-2, and EO-3) were produced with 0.30-0.50 wt.% C, 0.40-0.50 wt.% Si, 0.75-0.90 wt.% Mn, 1.00 wt.% Cr, and 0.12-0.21 wt.% La. The composition series was used as a comparative alloy-design set rather than as a single-factor La experiment.
- The EO alloys retained mechanical properties in the range required for structural comparison with cast steels. EO-3 exhibited the highest tensile strength within the EO series (480 MPa), whereas EO-2 showed the highest impact toughness (50 J/cm^2). No single EO composition maximized all mechanical characteristics simultaneously.
- The damping-related parameters differed substantially among the EO alloys. EO-3 showed the highest reported internal-friction value, 31.245 x 10^-4, compared with 18.281 x 10^-4 for EO-1 and 16.268 x 10^-4 for EO-2. The ordering of sound

levels did not follow the ordering of internal-friction values, confirming that these quantities should not be treated as equivalent indicators.
• EO-3 was selected for surface modification with a ceramic-metal nanostructured TiN-Ni coating. The direct paired comparison showed that the A-weighted impact sound level decreased from 70 dBA for uncoated EO-3 to 56 dBA for EO-3/CMNC, corresponding to a reduction of 14 dBA.
• The reported internal-friction parameter of EO-3 decreased after coating deposition, from 31.245 x 10^-4 to 14.281 x 10^-4. Therefore, the coating effect is better described as a pronounced modification of the vibroacoustic response and acoustic radiation rather than a simple increase in internal friction.
• The TiN-Ni coating exhibited a nanostructured, predominantly columnar morphology. Variation of Ni content was associated with refinement of TiN crystallites from approximately 100-110 nm to about 15 nm; at Ni contents below 12 at.% the metallic component was reported as X-ray amorphous, whereas higher Ni contents promoted TiNi formation and increased porosity.
• The combined results support a material-design strategy in which bulk composition and surface engineering are optimized together. Further verification should include a La-controlled alloy series, fully documented TiN-Ni deposition parameters, and paired frequency- and amplitude-dependent damping measurements to separate intrinsic material damping from changes in impact-acoustic radiation.

Acknowledgements: This research was funded by the Science Committee of the Ministry of Science and Higher Education of the Republic of Kazakhstan, grant number AP27511849 «Development of alloy steels with dissipative properties and their surface modification by deposition of nanostructured wear-resistant coatings for critical components in mechanical engineering».

REFERENCES

1. WHO, *Occupational noise: assessing the burden of disease from work-related hearing impairment at national and local levels*. Geneva: World Health Organization, 2004.
2. NIOSH, *Current Intelligence Bulletin 38: Vibration Syndrome*. DHHS (NIOSH) Publication No. 83-110; 1983.
3. International Labour Organization. *Protection of Workers against Noise and Vibration in the Working Environment*. Geneva: ILO, 1984.
4. L. Zhang, et al.: Journal of Alloys and Compounds, 931, 2023, 167547. https://doi.org/10.1016/j.jallcom.2022.167547
5. W. He, et al.: Journal of Alloys and Compounds, 1008, 2024, 176513. https://doi.org/10.1016/j.jallcom.2024.03.1001
6. W. He, Y. Yuan, J. Yan, Y. Huang, H. Peng, Y. Wen: Journal of Alloys and Compounds, 977, 2024, 173345. https://doi.org/10.1016/j.jallcom.2023.173345
7. J. Zhang, Y. Wang, Q. Luo, H. Peng, Y. Wen: Philosophical Magazine, 101(15), 2021, 1765–1781. https://doi.org/10.1080/14786435.2021.1939901
8. W. He, Q. Luo, H. Peng, Y. Wen: Materials Science and Technology, 36(12), 2020, 1329–1337. https://doi.org/10.1080/02670836.2020.1780002
9. L. Yu, Y. Ma, C. Zhou, H. Xu: International Journal of Solids and Structures, 42, 2005, 3045–3058. https://doi.org/10.1016/j.ijsolstr.2004.10.009
10. R. Akhter, A. Bendavid, P. Munroe: Applied Surface Science, 573, 2022, 151536. https://doi.org/10.1016/j.apsusc.2022.151536
11. R. Akhter, A. Bendavid, P. Munroe: Applied Surface Science, 590, 2022, 153107. https://doi.org/10.1016/j.apsusc.2022.153107
12. V.N. Zhuravlev, O.I. Nikolaeva: *Machine-building steels. Handbook*. 3rd ed. Moscow: Machine-building, 1981, 391 p.
13. E.B. Utepov, D.K. Suleev, T.E. Utepov, et al.: *Scientific foundations for the creation of "quiet" alloys (problems of acoustic ecology).* Almaty: LLP Print, 2000, 332 p.
14. R.Zh. Abuova, et al.: Science and Technology of Kazakhstan. 2025(4), 2025, 170–183.
15. R. Chen, Z. Wang, F. Zhu, et al.: Journal of Alloys and Compounds, 824, 2020, 153849. https://doi.org/10.1016/j.jallcom.2020.153849
16. N. Mao, W. Yang, D. Chen, et al.: Materials, 15(22), 2022, 7952. https://doi.org/10.3390/ma15227952
17. A. Granato, K. Lücke: Journal of Applied Physics, 27(6),1956, 583–593. https://doi.org/10.1063/1.1722436